The EMBO Journal Vol.16 No.2 pp.211–220, 1997

Molecular structure of the sarcomeric M band: mapping of titin and myosin binding domains in myomesin and the identification of a potential regulatory phosphorylation site in myomesin

Wolfgang M.J.Obermann[1], Mathias Gautel[2], Klaus Weber[1] and Dieter O.Fürst[1,3,4]

[1]Max-Planck-Institute for Biophysical Chemistry, Department of Biochemistry, PO Box 2841, D-37077 Göttingen, [2]European Molecular Biology Laboratory, Biological Structures and Biocomputing Program, D-69012 Heidelberg and [3]University of Potsdam, Department of Cell Biology, Lennéstrasse 7a, D-14471 Potsdam, Germany

[4]Corresponding author

The M band of sarcomeric muscle is a highly complex structure which contributes to the maintenance of the regular lattice of thick filaments. We propose that the spatial coordination of this assembly is regulated by specific interactions of myosin filaments, the M band protein myomesin and the large carboxy-terminal region of titin. Corresponding binding sites between these proteins were identified. Myomesin binds myosin in the central region of light meromyosin (LMM, myosin residues 1506–1674) by its unique amino-terminal domain My1. A single titin immunoglobulin domain, m4, interacts with a myomesin fragment spanning domains My4–My6. This interaction is regulated by phosphorylation of Ser482 in the linker between myomesin domains My4 and My5. Myomesin phosphorylation at this site by cAMP-dependent kinase and similar or identical activities in muscle extracts block the association with titin. We propose that this demonstration of a phosphorylation-controlled interaction in the sarcomeric cytoskeleton is of potential relevance for sarcomere formation and/or turnover. It also reveals how binding affinities of modular proteins can be regulated by modifications of inter-domain linkers.

Keywords: myomesin/myosin binding/phosphorylation/sarcomere/titin binding

Introduction

The impressively regular and stable organization of thick and thin filament lattices in the sarcomeres of cross-striated muscles cannot be explained by the self-assembly properties of their major constituents, actin and myosin. Instead, it is brought about by a cytoskeletal framework whose complexity was only appreciated recently (see, e.g., review by Small *et al.*, 1992). The most obvious structures involved in the regular packing of contractile filaments are the Z discs and M bands, which organize thin and thick filaments, respectively. The only component identified to date that could integrate both structures is the giant protein titin (also called connectin) together with its associated proteins (for a recent review, see Fürst and Gautel, 1995).

A small group of proteins specifically located in the M band is known. Apart from the ATP-regenerating enzyme MM-creatine kinase, three structural proteins have been established in this region: M-protein (Masaki and Takaiti, 1974), myomesin (Grove *et al.*, 1984) and titin (Nave *et al.*, 1989). M-protein originally was characterized biochemically as a myosin-associated protein (Masaki and Takaiti, 1974; Trinick and Lowey, 1977) and myomesin was identified as a contaminant in M-protein preparations by using monoclonal antibodies (mAbs) (Grove *et al.*, 1984). The function of both proteins remained largely enigmatic. The finding that both myomesin and M-protein also bind to titin suggests that they have essentially cytoskeletal functions (Nave *et al.*, 1989; Vinkemeier *et al.*, 1993). While myomesin is found in all striated muscle fibres examined, M-protein is restricted to fast skeletal and cardiac fibres (Grove *et al.*, 1985, 1987).

A structural model describing the exact disposition of titin, myomesin and M-protein in the M band was only introduced recently (Obermann *et al.*, 1996). The availability of cDNA information for titin, myomesin and M-protein enabled the production of a panel of specific and sequence-assigned antibodies and the subsequent localization of the respective epitopes at the sarcomere level by electron microscopy. In this model, the carboxy-terminal end of titin spans the central M1 line and reaches ~60 nm into the other sarcomere half. While myomesin was also implied to bridge the M1 line and to be arranged largely in an antiparallel and staggered fashion, M-protein could bridge the thick filaments primarily in a perpendicular orientation (Obermann *et al.*, 1996). This model puts certain constraints on protein–protein interactions necessary to achieve the three-dimensional structure of the M band. We approached this problem by producing a series of recombinant fragments of myomesin, of the LMM portion of myosin and of the 250 kDa carboxy-terminal region of titin, and have used these to search for mutual binding sites. The results are in good agreement with the previously proposed model. The possibility of regulating at least one of the binding sites by phosphorylation invites some speculation on its function during sarcomere formation and/or turnover.

Results

A novel phosphorylation site in the loop between domains My4 and My5 of myomesin

In the myomesin molecule, a unique amino-terminal domain (138 residues) is followed by 12 repeat domains which reflect immunoglobulin cII and fibronectin type III domains respectively (Vinkemeier *et al.*, 1993; Figure 1). Although computer analyses of the human sequence did not indicate specific target sites for protein kinases (Vinkemeier *et al.*, 1993), we observed that the phosphorylation-dependent mAb NE-14, which is directed against porcine neurofilament H protein (Shaw *et al.*, 1984), shows cross-reactivity

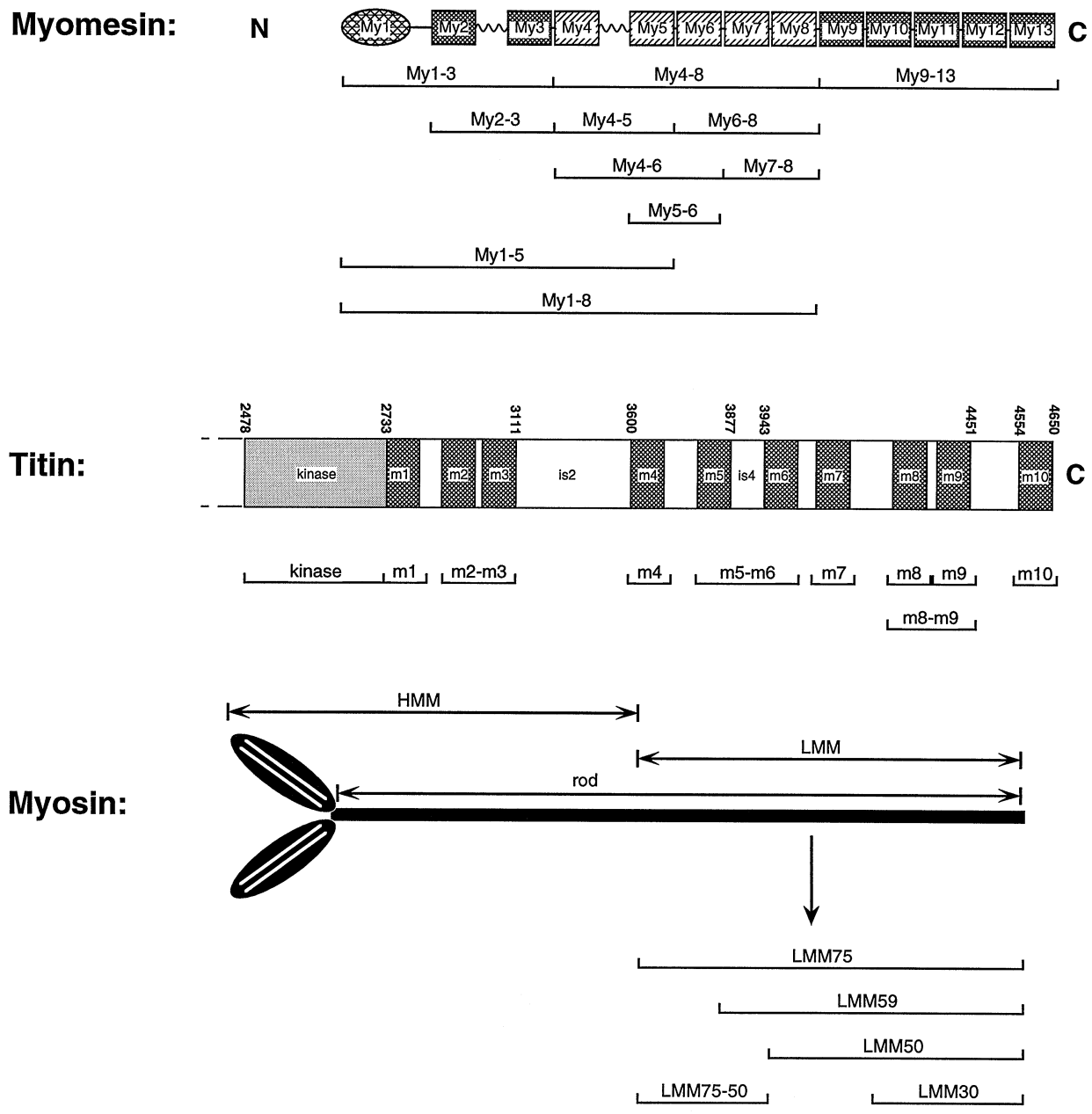

Fig. 1. Schematic representation of domain organizations for myomesin, for the carboxy-terminal 250 kDa region of titin and for myosin. The presentation emphasizes the modular construction of myomesin and titin from repetitive immunoglobulin cII (cross-hatched rectangles) and fibronectin type III repeats (striped rectangles) interspersed by unique sequence stretches of varying length (is stands for insertion). The recombinant constructs used for mapping of binding sites are indicated. The location of the most prominent proteolytic fragments of myosin is shown in the lower panel. Brackets give the borders of the recombinant LMM constructs used in this study.

with purified bovine myomesin. The corresponding phosphorylation site locates to the ~60 carboxy-terminal residues of myomesin (Obermann *et al.*, 1995). To search for kinases acting on myomesin, the purified protein was incubated with three distinct protein kinases in the presence of [^{32}P]ATP. While cAMP-dependent protein kinase A (PKA) was able to phosphorylate myomesin (Figure 2A), protein kinase C and casein kinase showed no reaction (data not shown). For a preliminary mapping of the phosphorylation site, we used the limited proteolysis procedure with endoproteinase Lys-C which generates two myomesin fragments with M_rs of 116 and 109 kDa, respectively. Since both fragments were shown by direct protein sequencing to start with Ser479, their mass difference must reside in a carboxy-terminal end that is ~60 residues shorter in the lower molecular mass fragment (Obermann *et al.*, 1995). If, as we assumed, the PKA phosphorylation site was identical to the site previously identified in this region by mAb NE-14, only the higher molecular mass band should be phosphorylated. Figure 2A (lane 2) shows an autoradiograph of the Lys-C limited digest of bovine myomesin previously radioactively phosphorylated by PKA. Surprisingly both fragments are radioactively labelled. Thus, myomesin shows an unexpected phosphorylation site which must lie between Ser479 and the last residue common to the two fragments.

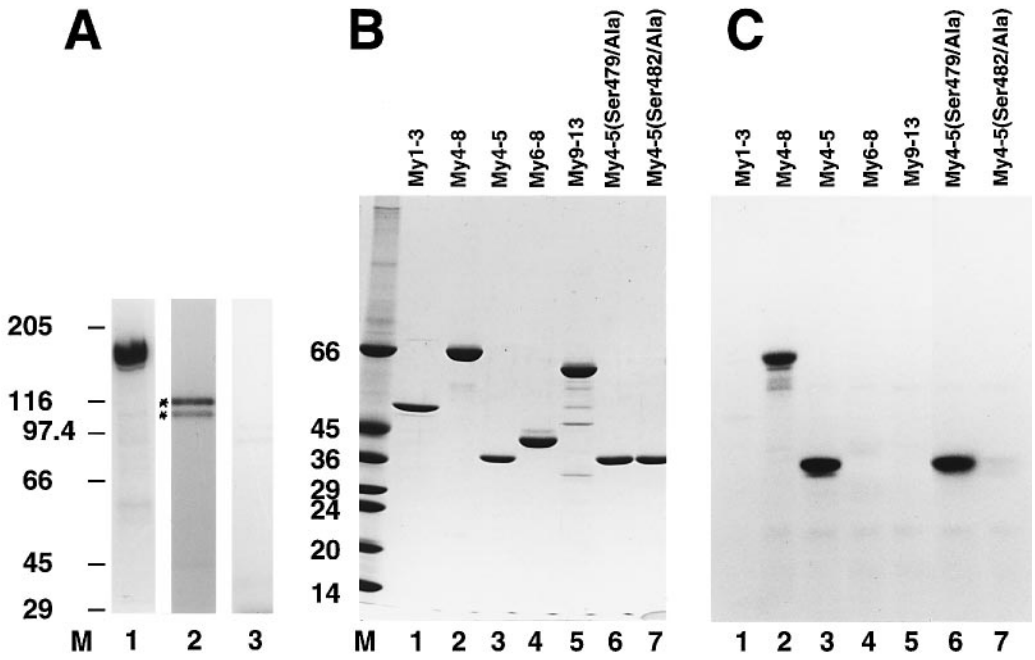

Fig. 2. Phosphorylation of purified myomesin and its recombinant fragments. (**A**) Myomesin purified from bovine skeletal muscle (lane 1) was incubated with PKA, digested with endoproteinase LysC (lane 2) and with trypsin (lane 3) and subsequently analysed by 4–12% SDS–PAGE (see Materials and methods). Corresponding autoradiographs are shown. Note that whole myomesin and both major fragments generated by endoproteinase LysC treatment (indicated by asterisks) are phosphorylated, while the trypsin fragment is not. (**B**) A 6–20% SDS–PAGE analysis of purified recombinant myomesin fragments My1–3 (lane 1), My4–8 (lane 2), My4–5 (lane 3), My6–8 (lane 4), My9–13 (lane 5), My4–5 (Ser479Ala) (lane 6) and My4–5 (Ser482Ala) (lane 7). For domain structure of myomesin see Figure 1. M = molecular mass standards (numbers indicate $M_r \times 10^3$). (**C**) Autoradiographs of samples corresponding to lanes B1–B7 after phosphorylation with PKA and ^{32}P-labelled ATP. Note that My4–8 and My4–5 are phosphorylated (lanes C2 and C3) while My1–3 (lane C1), My6–8 (lane C4) and My9–13 (lane C5) are unlabelled. The Ser479Ala mutant of My4–5 is phosphorylated (lane C6). Phosphorylation of My4–5 is abolished completely in the Ser482Ala mutant (lane C7). Thus Ser482 is the PKA phosphorylation site of myomesin.

For a more precise mapping of the PKA phosphorylation site, we used a series of overlapping myomesin constructs amplified from the human cDNA by PCR and cloned into the modified bacterial expression vector pET described before (Obermann *et al.*, 1996). Corresponding recombinant proteins were overexpressed in *Escherichia coli* and purified under native conditions making use of their carboxy-terminal $(His)_6$ tag to facilitate purification. Figure 2B shows the purity of the recombinant myomesin fragments used in the phosphorylation studies and their location with respect to the domain organization of myomesin is given in Figure 1. Recombinant fragments were treated with PKA and ATP under standard assay conditions. SDS–PAGE and corresponding autoradiographs (Figure 2B and C) showed that myomesin My4–5 and larger fragments containing these two domains (see My4–8) are phosphorylated efficiently, while My1–3, My6–8 and My9–13 are not substrates for PKA. Phosphoamino acid analysis of radiolabelled My4–5 and myomesin showed that PKA phosphorylation occurs exclusively on serine (Figure 3A). Closer inspection of the sequence of My4–5 in the human myomesin sequence (Vinkemeier *et al.*, 1993) hinted at the rather long insertion connecting these two FN domains (see also Figure 1). This region of ~35 residues harbours a sequence containing four basic residues, two serines and two prolines, KARLKSRPSAP (residues 474–484), which is more likely to be accessible than the serines in the tightly packed β-barrels of the repeat domains. Therefore, a synthetic peptide EKARLKSRPSAPWTGQ (residues 473–488) covering this region was tried as a PKA substrate. This peptide is phosphorylated efficiently by PKA. Since this sequence describes a novel target site for PKA, the kinetics of the phosphorylation reaction were compared with the kinetics of the liver pyruvate kinase peptide LRRASLG ('kemptide'), which is an excellent substrate for PKA with a K_m of 16 μM and a V_{max} of 20.2 μmol/min/mg (Kemp *et al.*, 1977). Table I shows that the apparent K_m value of kemptide measured under our assay conditions was nearly identical to the published value. The K_m of the myomesin peptide EKARLKSRPSAPWTGQ was 532 μM. The V_{max} was not obtained in absolute numbers, since the enzyme concentration in the commercially available sample of PKA and in muscle extracts could not be measured. Instead, the numbers of our measurements in Table I indicate relative units. Thus the V_{max} of the myomesin peptide phosphorylation reaction is ~50% of that of the kemptide reaction. Reverse phase HPLC (Figure 3B) shows a clear shift of the elution volume of the peptide after phosphorylation. This mobility shift indicates that under standard assay conditions the peptide is converted quantitatively into the phosphorylated form. Phosphorylation of the peptide was, as in My4–5, serine specific (data not shown).

To decide which serine in residues 474–484 is the target site for PKA, two constructs comprising myomesin My4–5 were made and either serine 479 or 482 was substituted by alanine. The constructs were expressed in *E.coli* and the two recombinant myomesin fragments carrying a single point mutation were purified in the native state. Subsequent phosphorylation assays with PKA monitored

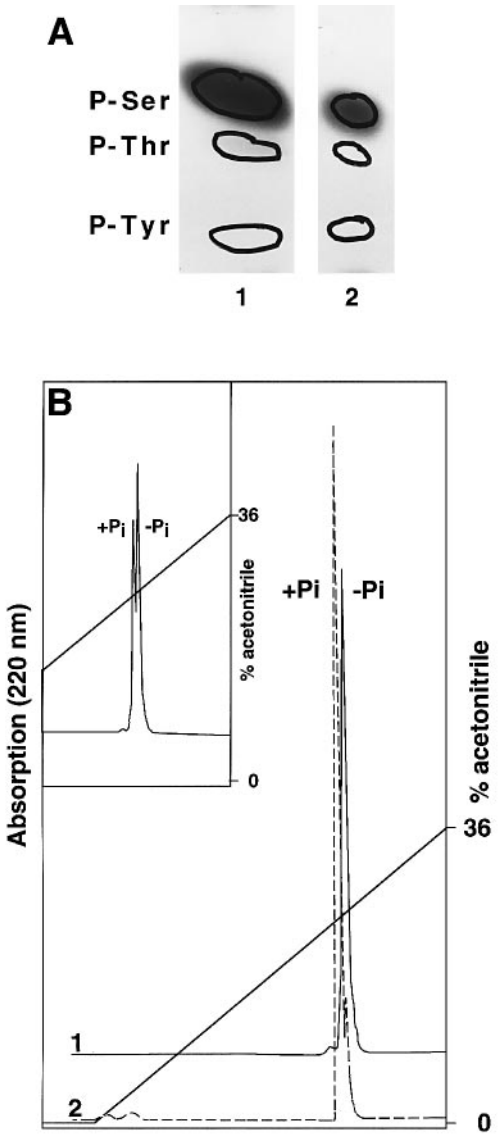

Fig. 3. Phosphoamino acid analysis and HPLC analysis of the phosphorylated peptide. (**A**) Phosphoamino acid analysis of the recombinant myomesin fragment My4–5 (lane 1) and of native myomesin from bovine skeletal muscle (lane 2) after phosphorylation with PKA. The positions of marker amino acids are indicated. (**B**) Phosphorylation of the synthetic peptide EKARLKSRPSAPWTGQ (myomesin residues 473–488) by PKA analysed by HPLC (see Materials and methods). Note the small but significant difference in elution volumes for the unphosphorylated ($-P_i$; curve 1) and phosphorylated ($+P_i$; curve 2) peptide. Co-chromatography of both species (insert) clearly shows separation into two peaks.

by SDS–PAGE and autoradiography (Figure 2B and C) demonstrated that My4–5 (Ser479/Ala) is still phosphorylated while My4–5 (Ser482/Ala) is no longer a substrate of PKA. Thus myomesin Ser482 is the phosphorylation site for PKA.

Myomesin is phosphorylated by skeletal muscle extracts

A series of extracts from muscle tissues was tested for their ability to incorporate radioactive phosphate into myomesin. The results resembled the *in vitro* observations with PKA. Native myomesin purified from bovine skeletal muscle and the recombinant fragments listed in Figure 2

Table I. Phosphorylation of synthetic peptides by PKA

Peptide sequence	Apparent K_m (μM)	V_{max}
LRRASLG	16	20.2 mmol/min.mg
LKRASLG	1400	17.1 mmol/min.mg
LRKASLG	260	16.9 mmol/min.mg
LRRASLG	14	266.4 c.p.m./min
EKARLKSRPSAPWTGQ	532	130.9 c.p.m./min

The upper part of the table gives apparent K_m and V_{max} values reported for the well characterized PKA substrate kemptide LRRASLG and variations of this sequence (Kemp *et al.*, 1977). The lower part compares measured values for kemptide and the myomesin peptide EKARLKSRPSAPWTGQ (see Results). Phosphorylation reactions were performed as described in Materials and methods. Peptide sequences are given in column 1.

were phosphorylated as described above for purified PKA (data not shown). No difference was observed with respect to the state of differentiation of the muscle tissue from which the extract was derived. Thus the degree of phosphorylation of the myomesin My4–5 fragment was the same with extracts from rat fetal (gestation day 14), neonatal and adult rat psoas muscle (results not shown). The ability of these extracts to phosphorylate Ser482 in the My4–5 fragment was also characterized in the presence of the PKA substrate kemptide (Kemp *et al.*, 1977). It resulted in a complete inhibition of the phosphorylation of the myomesin fragment. Similarly, the presence of the regulatory subunit of PKA also led to complete inhibition of the phosphorylation of the myomesin fragment (results not shown). In contrast, addition of EGTA or Ca^{2+}/calmodulin to phosphorylation assays did not affect incorporation of radioactive phosphate into myomesin My4–5. We conclude, therefore, that myomesin phosphorylation by muscle extracts is probably the result of PKA or an enzyme closely related to PKA.

Interaction of myomesin with titin is modulated by phosphorylation of Ser482

Overlapping myomesin fragments spanning the entire molecule and nine domains from the carboxy-terminal (M band) region of titin (see scheme in Figure 1) were expressed in *E.coli* and purified by Ni–NTA chelate affinity chromatography followed by ion-exchange chromatography. Figure 4 documents the purity of the panels of purified myomesin fragments (My1–8, My1–5, My4–5, My4–8, My5–6, My9–13, My4–6 and My7–8) and titin fragments (m1, m2–m3, m4, m5–m6, m7, m8, m8–m9, m9, m10 and the titin kinase domain) by SDS–PAGE. A solid phase overlay assay was used to investigate the myomesin–titin interaction (Figure 5). Interestingly, m4 is the only titin domain which shows highly selective interaction with myomesin fragments My1–8 and My4–8. Since the titin fragment m5–m6, which lies next to m4 (see domain structure in Figure 1) lacked myomesin binding (Figure 5), we also used m5–m6 after phosphorylation by cdc2 kinase in the overlay assay. Again, no binding of myomesin fragments was observed (Figure 5).

For a more precise mapping of the titin m4 binding site within the five domains of myomesin fragment My4–8, a series of constructs representing different portions of this region were made. Surprisingly, all of the myomesin

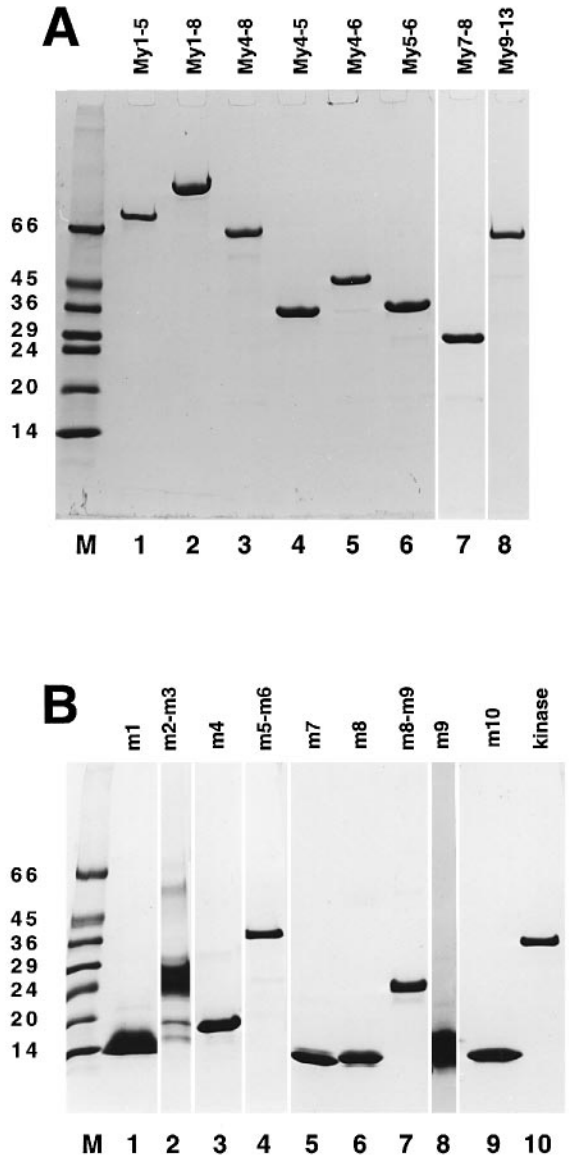

Fig. 4. SDS–PAGE analysis of purified recombinant myomesin and titin fragments used in binding studies. A 6–20% gradient gel was used (M = molecular mass standards). (**A**) Myomesin fragments My1–5 (lane 1), My1–8 (lane 2), My4–8 (lane 3), My4–5 (lane 4), My4–6 (lane 5), My5–6 (lane 6), My7–8 (lane 7) and My9–13 (lane 8). (**B**) Titin fragments m1 (lane 1), m2–m3 (lane 2), m4 (lane 3), m5–m6 (lane 4), m7 (lane 5), m8 (lane 6), m8–m9 (lane 7), m9 (lane 8), m10 (lane 9) and titin kinase (lane 10). For the domain structure of myomesin and the 250 kDa carboxy-terminal region of titin see Figure 1.

fragments comprising only two FN domains lost the ability to interact with the titin domain m4 (Figure 5; for domain structure see Figure 1). In contrast, myomesin fragment My4–6, which covers the first three FN domains, retained binding to titin (Figure 5). The results were the same whether titin domains were spotted onto nitrocellulose and overlayed with myomesin fragments, or the reverse order was used. This demonstrates the selectivity and specificity of the solid phase overlay assay used.

Since myomesin fragment My4–6 contains the PKA phosphorylation site identified above, it was particularly interesting to see whether phosphorylation of Ser482 would influence the binding to titin m4. Therefore, the binding assay was repeated using the myomesin fragment My4–6 either directly or after PKA phosphorylation (Figure 5B). Interestingly, phosphorylation almost completely abolished the binding of My4–6 to titin domain m4.

The amino-terminal head domain of myomesin binds to myosin; location of the myomesin binding site on the myosin rod

A previous study reported binding of myomesin to the LMM portion of myosin (Obermann *et al.*, 1995). For a more detailed mapping of the binding sites in both proteins, a series of recombinant myomesin fragments, and several proteolytic and recombinant derivatives of myosin were made. Figure 6A and B shows the purity of these derivatives. Again a solid phase overlay assay was used to delineate the sites of interaction. While myomesin fragments My2–3, My4–8 and My9–13 lacked binding to LMM, the myomesin fragment My1–3, which contains the head domain, showed a concentration-dependent binding to LMM (Figure 6C). This finding suggests that the unique amino-terminal head portion of the myomesin molecule bears the myosin binding site. The location of this binding site within the myomesin molecule is also indicated in the schematic representation given in Figure 7.

In the same way, different myosin derivatives were used to map the myomesin binding site on the rod portion of myosin with greater precision. While proteolytic myosin rod, proteolytic and recombinant LMM as well as LMM 59 and LMM 50 were recognized by the myomesin fragment My1–3, LMM 50–75 and LMM 30 failed to bind myomesin My1–3 (Figure 6C). We conclude, therefore, that the myosin binding site on the myosin heavy chain is confined to the 169 amino acids between residues 1506 and 1674 located in the central part of LMM (numbers refer to the amino acid sequence of rabbit fast skeletal muscle myosin heavy chain; see Maeda *et al.*, 1987).

Discussion

As a ubiquitous protein of vertebrate sarcomeric M bands, myomesin can be supposed to play a key role in establishing this complex structure. At the level of isolated proteins, it has been established that myomesin binds to both titin (Nave *et al.*, 1989) and myosin (Obermann *et al.*, 1995). Thus, myomesin may act as a cross-linker connecting the M band end of titin with myosin thick filaments. It is important, therefore, to map the respective binding sites in detail and to search for possible regulatory mechanisms.

Our recent biochemical characterization of myomesin purified from bovine skeletal muscle revealed phosphorylation present within the carboxy-terminal ~60 residues of the polypeptide (Obermann *et al.*, 1995). In an effort to search for the corresponding protein kinase, we now found a second, novel phosphorylation site. The combination of several approaches clearly established that Ser482 is the only residue that is phosphorylated specifically *in vitro* by PKA (Figures 2 and 3). This serine lies in the region connecting myomesin domains My4 and My5 (Figure 1) and is situated in the sequence KARLKSRPS*AP (residues 474–484; Vinkemeier *et al.*, 1993). While it is more difficult to envisage that a particular sequence located

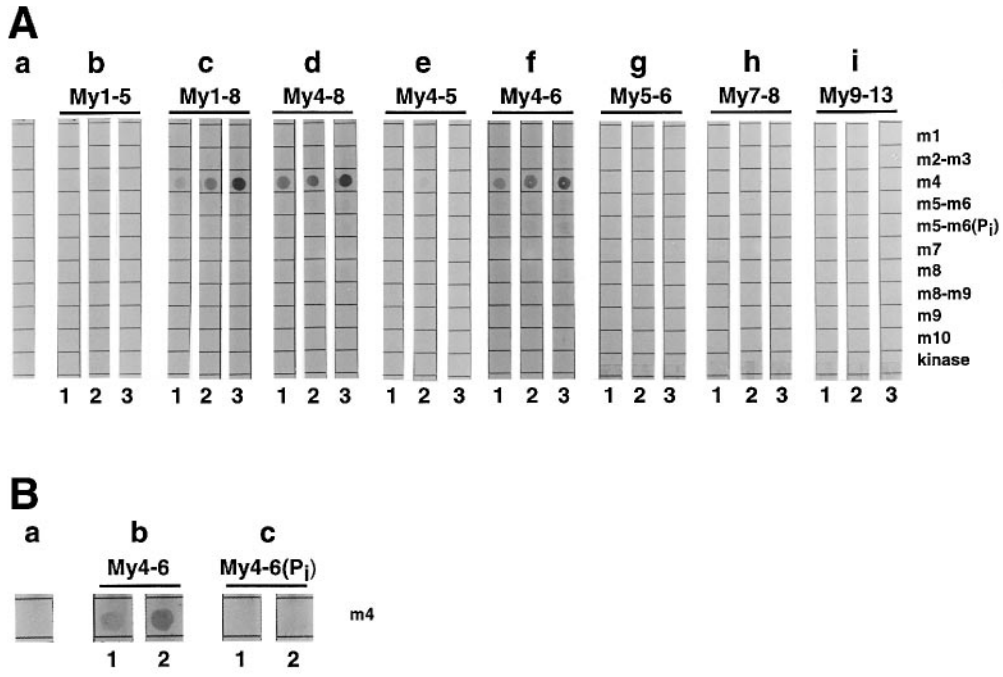

Fig. 5. Interaction of myomesin fragments with M band titin. In (**A**), 0.2 μg per domain of titin fragments m1, m2–m3, m4, m5–m6, m5–m6(P_i), m7, m8, m8–m9, m9, m10 and titin kinase were spotted on nitrocellulose sheets and incubated with increasing concentrations (1 = 0.2 μM, 2 = 0.6 μM, 3 = 1.8 μM) of myomesin fragments My1–5 (b), My1–8 (c), My4–8 (d), My4–5 (e), My4–6 (f), My5–6 (g), My7–8 (h) and My9–13 (i). (a) Control without myomesin in the incubation solution. Binding of recombinant myomesin fragments carrying the T7 tag was detected by T7 tag-specific antibody (for details see Materials and methods). Only My1–8, My4–8 and My4–6 bind to titin (for domain structures of myomesin and titin see Figure 1). This binding of myomesin to titin is restricted to titin m4. In (**B**), it is shown that the binding affinity of myomesin My4–6 for titin m4 is reduced strongly by phosphorylation of myomesin at Ser482. Titin m4 (0.2 μg) was spotted onto nitrocellulose sheets and overlayed with increasing concentrations (1 = 0.2 μM, 2 = 0.6 μM) of myomesin My4–6 (b) or with the phosphorylated species My4–6(P_i) (c) respectively. (a) Control without myomesin fragment in the incubation solution. Phosphorylation of myomesin My4–6 by PKA strongly reduces its binding affinity for titin m4.

within any of the densely packed Ig or FN repeat domains of myomesin would be a likely kinase target site, most of the basic residues in the loop sequence can be expected to be exposed to the surrounding medium and therefore to be a part of a kinase site. This particular site in myomesin also describes a novel target sequence for PKA whose preferred targets show two basic residues separated by one residue from a serine or threonine (Pearson and Kemp, 1991). In the myomesin sequence, four lysine/arginine residues provide a basic environment amino-terminal to the phosphorylatable serine. Correspondingly, we find that a synthetic peptide spanning residues 473–488 is phosphorylated quantitatively by PKA under standard conditions. The apparent K_m and V_{max} values of this reaction (see Table I) indicate that myomesin is indeed capable of serving as a PKA target comparable with other substrates (Pearson and Kemp, 1991). When these values are compared, one has to take into account that most of the substrates characterized so far are soluble proteins. While for these proteins low K_m values are essential to enable efficient phosphorylation in the cytosol, the high local concentration of myomesin in the M band may allow for higher K_m values.

The possible significance of this phosphorylation site for the *in vivo* situation during myofibrillogenesis is emphasized by the observation that extracts of various muscle tissues of different developmental stages (from gestation day 16 rat embryos to adult) exhibit similar kinase activities on purified myomesin or its fragment My4–5 which harbours Ser482. It remains to be seen whether PKA phosphorylation of myomesin temporarily suppresses myomesin interactions during the early stages of myofibrillogenesis *in vivo*.

In this context, the localization of a titin binding site in the myomesin molecule established in this study is particularly interesting. Only fragments containing at least the three FN domains My4–6 exhibited binding to the titin Ig domain m4 (Figure 5). Single domains or pairs of neighbouring domains from My4–5 were not reactive in the solid phase overlay assay. This observation seems to resemble the situation found in the interaction between titin and cardiac C-protein, where also a construct consisting of at least three C-protein domains was identified as the minimal requirement for titin binding (Freiburg and Gautel, 1996). It appears that a larger number of weak but cooperative interactions is necessary to establish the stable complexes of titin with its various associated proteins that can be observed *in vivo*. It is probably essential for the ordered sequence of events during sarcomeric contraction–relaxation cycles that stable connections between contractile and cytoskeletal elements are retained. Most intriguing in this context is the finding that phosphorylation of a single serine residue (Ser482) within the myomesin binding site for titin resulted in an almost complete inhibition of binding (Figure 5B). Apparently the phosphorylation state of Ser482, which is located in the loop connecting myomesin domains My4 and My5, regulates the three-dimensional arrangement of the three titin binding domains (My4–6) in a rather complex manner. The *in vitro* results invite some speculation on the molecular mechanisms of

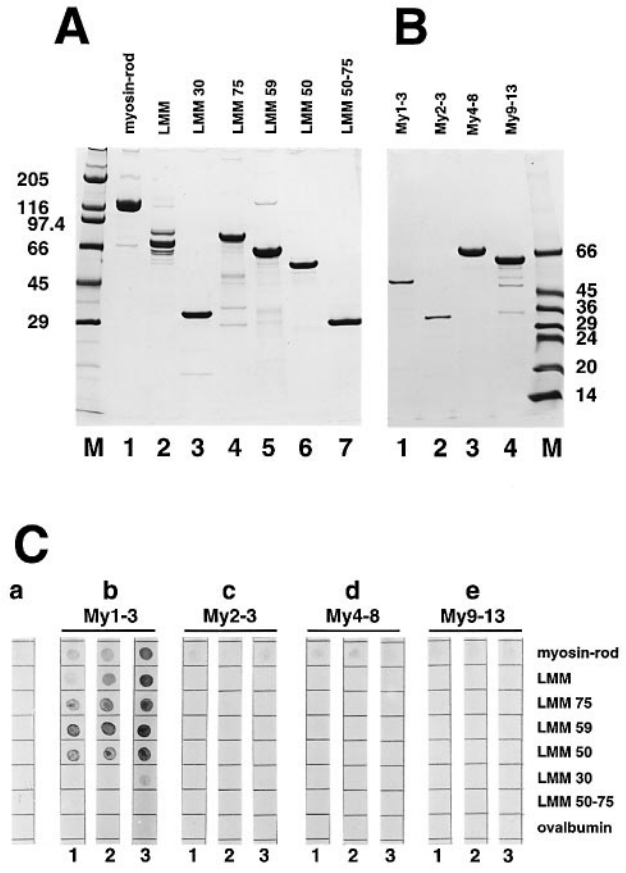

Fig. 6. Binding of recombinant myomesin fragments to proteolytic and recombinant derivatives of myosin. SDS–PAGE analysis of purified derivatives of myosin (**A**) and myomesin (**B**). Gradient gels of 6–20% were used. M = molecular mass standards in kDa. The myosin derivatives in (A) are myosin rod (lane 1), proteolytic LMM (lane 2), LMM 30 (lane 3), LMM 75 (lane 4), LMM 59 (lane 5), LMM50 (lane 6) and LMM 50–75 (lane 7). The myomesin fragments in (B) are My1–3 (lane 1), My2–3 (lane 2), My4–8 (lane 3) and My9–13 (lane 4). For the domain structures of myosin and myomesin see Figure 1. (**C**) The results of binding assays. The same amounts (~1 μg) of myosin rod, proteolytic LMM, LMM 75, LMM 59, LMM 50, LMM 30, LMM 50–75 and ovalbumin serving as control were spotted on nitrocellulose filters and overlaid with increasing concentrations (1 = 0.1 μM, 2 = 0.5 μM, 3 = 2.5 μM) of myomesin fragments My1–3 (b), My2–3 (c), My4–8 (c) and My9–13 (e). (a) Control without protein. Binding of myomesin fragments carrying the carboxy-terminal EEF tag was detected with monoclonal antibody YL1/2, which specifically recognizes this tag. Note the specific binding of myomesin fragment My1–3 to all myosin fragments which contain at least the central portion of LMM (myosin heavy chain residues 1506–1674; Figure 1). Since myomesin fragment My2–3 lacks the myosin binding of My1–3, the myosin binding site of myomesin locates to the amino-terminal head domain.

sarcomere formation, regeneration and turnover. In all cases, local signals for either the formation or the breakdown of certain complexes are needed. These could be provided by the phosphorylation/dephosphorylation of myomesin which in turn regulate its binding to titin. Likewise, the formation of stable links between titin molecules from neighbouring half sarcomeres might stabilize the cytoskeletal structures during myofibrillogenesis. The physiological role of myomesin phosphorylation in myofibril assembly remains now to be explored in the cellular context.

Solid phase overlay assays also delineated the molecular region of myomesin involved in the previously detected binding of myosin (Obermann *et al.*, 1995). Since only constructs that contained at least myomesin domain My1 (i.e. the unique amino-terminal domain) exhibited binding (Figure 6), we conclude that this domain either comprises the myosin binding site *per se* or is an essential part of a larger binding site. Since we could not stably express the My1 domain alone, we presently cannot distinguish between these two possibilities. Finally, we were able to locate the myomesin binding site on the myosin rod to residues 1506–1674 of the myosin heavy chain (Figure 6C; see Results). For a schematic representation of the established binding sites along the myomesin molecule, see Figure 7A.

The binding data presented here are in good agreement with the structural model of the sarcomeric M band region proposed on the basis of immunoelectron microscopical localizations of defined epitopes of myomesin, M-protein and the carboxy-terminal 250 kDa region of titin (Obermann *et al.*, 1996; adopted in Figure 7B). The latter results have, for instance, suggested a particular arrangement of myomesin. While most of the myomesin domains seem organized parallel to the long axis of myofibrils, the amino-terminal domains My1–2 appear to bend towards the thick filament. This region, most likely My1, indeed contains a myosin binding site (see above). Likewise, the binding of myomesin domains My4–6 to titin domain m4 described above requires close proximity of these regions to allow for these interactions to occur. This proximity is given in the structural model of the M band based on immunoelectron microscopy of defined epitopes of myomesin and titin. Here titin m4 occurs at a distance of ~20–25 nm from the central M1 line, while the myomesin My4–6 region locates to a distance of ~18–25 nm from the M1 line (see Figure 7B).

Materials and methods

Expression of titin M line domains and myomesin fragments in E.coli

Original λ phage isolates containing cDNAs coding for the M band portion of human cardiac titin (Gautel *et al.*, 1993) were used as templates for PCR amplification (Saiki *et al.*, 1985) of domains (see below). PCR products were cloned into a modified pET23a vector (Novagen, Heidelberg, Germany), providing the resulting proteins with an EEF tag at their carboxy-termini. Since this tag is recognized by mAb YL1/2 (Wehland *et al.*, 1984), expression in *E.coli* BL21(DE3)pLysS was monitored by immunoblot analysis. Purification of the soluble recombinant proteins on Ni–NTA–agarose columns due to their oligohistidine tag followed standard protocols (Qiagen, Hilden, Germany).

Myomesin sequences were amplified by PCR (Saiki *et al.*, 1985) using the original λ phage isolates as templates (Vinkemeier *et al.*, 1993). PCR products were cloned into pET-23a derivatives. This provided the recombinant protein fragments with a carboxy-terminally located His_6 sequence and with either an amino-terminally located T7 tag or a carboxy-terminal EEF tag. After growth (LB medium supplemented with 2% glucose, 100 mg/l ampicillin and 34 mg/l chloramphenicol) and induction of *E.coli* BL21(DE3) LysS cells (Studier *et al.*, 1990) at OD_{600} = 1 with 0.1 mM IPTG at 25°C for 3 h, the cells were harvested and stored at –70°C. Pellets were resuspended and sonicated in buffer A (50 mM potassium phosphate pH 8.0, 500 mM KCl, 0.02% Tween-20, 5 mM 2-mercaptoethanol) containing 5 μM E64 and 1 mM phenylmethylsulphonyl fluoride (PMSF) as protease inhibitors. After centrifugation at 16 000 *g*, soluble recombinant proteins were enriched by metal chelate affinity chromatography. Briefly, protein solutions were applied onto Ni–NTA–agarose columns (Qiagen, Hilden, Germany), which were washed with buffer A and subsequently with buffer B (same as buffer A, except pH 6.0). Finally the recombinant proteins were

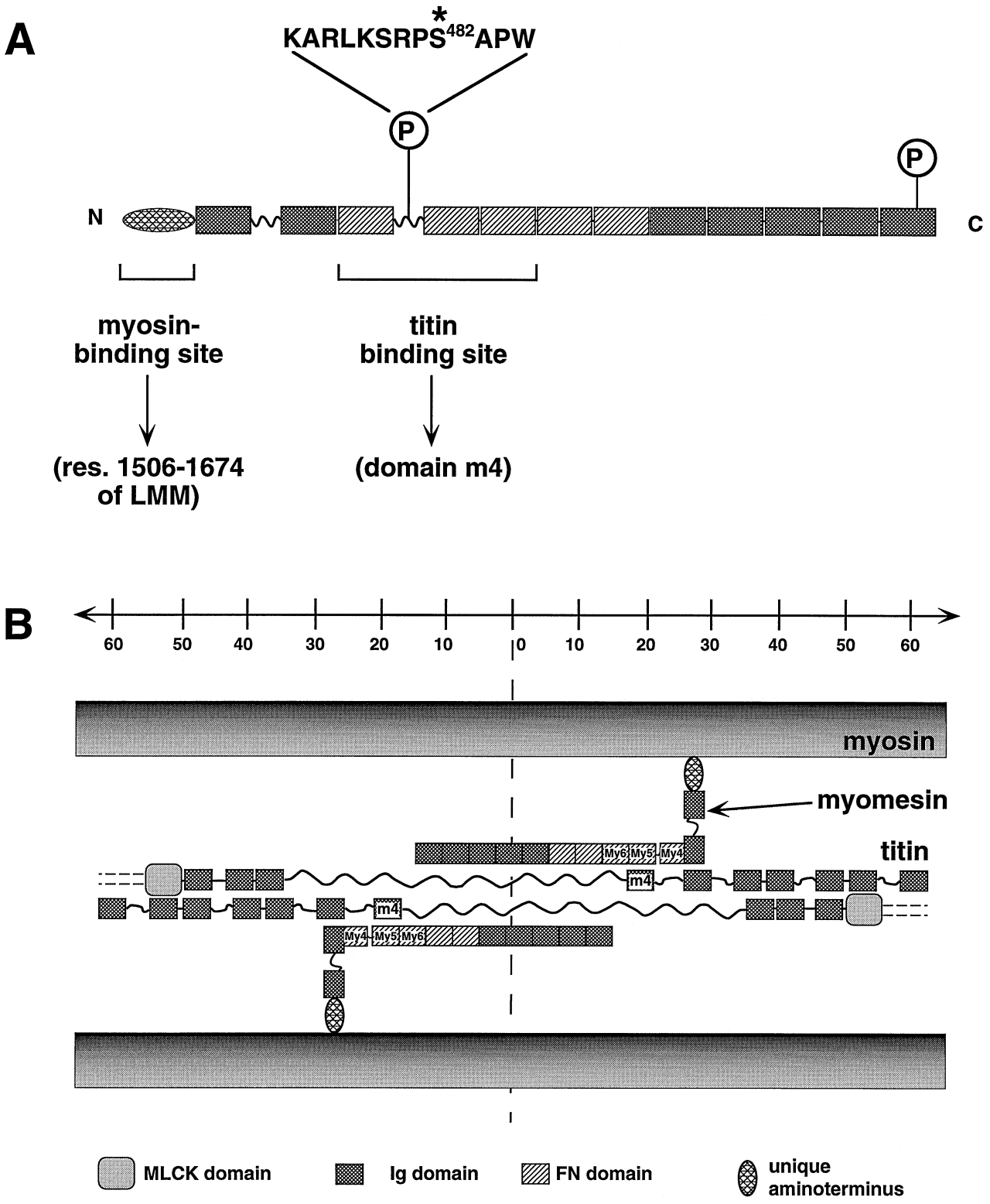

Fig. 7. Diagrams summarizing established binding sites in the myomesin molecule and arrangement of titin and myomesin in the M band. In (**A**), myosin and titin binding sites and phosphorylation sites in the myomesin molecule are illustrated. Cross-hatched and striped boxes indicate immunoglobulin cII domains and fibronectin type III, respectively. The amino acid sequence surrounding the PKA site (Ser482) in the insert between domains My4 and My5 is shown. Brackets indicate the myomesin domains in which binding sites were located (see text). The phosphorylation site at the carboxy-terminal end arises from an unknown protein kinase (Obermann *et al.*, 1995). (**B**) A schematic representation of the arrangement of titin and myomesin molecules in the M band compatible with immunoelectron microscopical results (Obermann *et al.*, 1996). At the top of the diagram, a scale bar indicates distances in the M band region in nm. Shading of domains is identical to (A). For domain designations also see Figure 1. Only two molecules of each kind are shown in order not to overburden the figure. Note the close proximity of myomesin domains My4–My6 to its binding partner, titin domain m4. For details see text. The scheme in (B) was modified from Obermann *et al.* (1996).

eluted with 500 mM imidazole in buffer B. After dialysis against buffer C [50 mM Tris–HCl, pH 7.9, 1 mM EDTA, 1 mM dithiothreitol (DTT)], recombinant proteins were purified further by ion-exchange chromatography on MonoQ or MonoS FPLC columns (Pharmacia, Uppsala, Sweden). The integrity of the purified proteins was monitored by N-terminal sequencing, the reaction with specific antibodies and the EEF tag-specific antibody YL1/2 (Wehland *et al.*, 1984).

Mutagenesis

Serine to alanine mutations were introduced into the myomesin My4–5 fragment by PCR amplification with mismatch oligonucleotides resulting in site-directed exchanges of serine to alanine codons following the method of Ausubel *et al.* (1987). Amplified fragments were subcloned into pET-23a-derived expression vectors (see above). DNA sequencing established the original sequence and the desired Ser–Ala exchanges.

Recombinant fragments of myosin

Different portions of rabbit fast skeletal muscle LMM were amplified by PCR using the original cDNA of rabbit myosin heavy chain-2/10 (Maeda *et al.*, 1987) as a template. Four constructs were designed, in which the carboxy-termini were identical with the end of the original clone (i.e. amino acid residue 1939). The amino-termini were situated at different points along the sequence of the myosin rod portion. This resulted in a series of 'shorter LMMs', which were designated according to their approximate molecular masses (in kDa): LMM75 (corresponding to residues 1284–1939 of the original clone; Maeda *et al.*, 1987), LMM59 (residues 1429–1939), LMM50 (residues 1506–1939) and LMM30 (residues 1675–1939). In addition, a further construct, called LMM75–50, was made. It corresponds to the amino-terminal portion of LMM and represents residues 1284–1505 of the myosin heavy chain sequence. PCR products were cloned into the pET-23a expression vector (Novagen, Heidelberg, Germany). Recombinant LMM fragments were expressed in *E.coli* BL21(DE3)pLysS and purified by two high salt–low salt extraction and precipitation cycles as described (Maeda *et al.*, 1989). All recombinant LMM fragments formed normal paracrystals as judged by electron microscopic inspection after negative staining (Maeda *et al.*, 1989).

Preparation of native proteins from bovine skeletal muscle

Myosin rod and LMM were prepared from bovine skeletal muscle by proteolytic cleavage with α-chymotrypsin as described by Margossian and Lowey (1982). Purification of bovine skeletal muscle myomesin and its proteolytic fragments obtained by endoproteinase Lys-C and trypsin have been described (Obermann *et al.*, 1995).

Phosphorylation of proteins and synthetic peptides

Purified myomesin, its proteolytic fragments and recombinant myomesin fragments were added at a final concentration of 0.2 μg/μl to 20 μl of assay buffer (50 mM MES pH 6.9, 100 mM KCl, 2 mM $MgCl_2$). Phosphorylation reactions were at 30°C for 30 min with 1 U of protein kinase A from porcine heart (Sigma) or 1 μl of muscle extract and 1 μCi of [γ-^{32}P]ATP (3000 Ci/mmol, Amersham). After addition of sample buffer (Laemmli, 1970) and heating at 65°C for 10 min, polypeptides were analysed by 4–12 or 6–20% SDS–PAGE. Autoradiography was at –80°C with intensifying screens.

For the *in vitro* phosphorylation of titin M5–M6, recombinant titin fragment M5–M6, containing the KSP repeats of the M band region of titin (Gautel *et al.*, 1993), was expressed solubly and purified as described above. The purified protein was incubated in 100 μl of assay buffer (25 mM HEPES pH 7.2, 10 mM $MgCl_2$, 1 mM EGTA, 1 mM DTT, 0.2 mM ATP) at 37°C for 30 min with recombinant cdc2- (New England Biolabs) or ERK-2 (Stratagene) SP-directed protein kinases, containing final concentrations of 0.1 mg/ml of the expressed substrate protein. Maximally, 2 mol/mol of phosphate could be incorporated as judged by parallel assays labelled with [γ-^{32}P]ATP and quantitation by liquid scintillation as described by Gautel *et al.* (1993). This indicates that in the presence of the flanking Ig domains, not all previously described SP phosphorylation sites are fully accessible.

Synthetic peptides were phosphorylated for kinetic experiments essentially as described by Kemp *et al.* (1977). Briefly, the reaction mixture (total volume 70 μl) contained the respective peptide at concentrations ranging from 0.1 to 1 mM in the following solution: 10 μCi [γ-^{32}P]ATP (0.5 mM), 62.5 mM MES, pH 6.9, 12.5 mM magnesium acetate, 0.25 mM EGTA and either protein kinase A (catalytic subunit, Boehringer, Mannheim, Germany) or muscle extracts prepared as described below. After incubation at 37°C for 0, 1, 2, 5, 10 and 15 min, 8 μl aliquots were removed from the reaction and the phosphorylated peptides were separated from [γ-^{32}P]ATP by the phosphocellulose binding technique described by Casnellie (1991). Apparent K_m and V_{max} values were determined by fitting the data of a double reciprocal Lineweaver–Burk plot to the Michaelis–Menten equation using the method of least squares.

Phosphoamino acid analysis

^{32}P-Labelled protein was recovered from sample buffer by the method of Wessel and Flügge (1984), dried and hydrolysed in 6 M HCl at 110°C for 2 h. After lyophilization, the hydrolysate was dissolved in 10 μl of H_2O and applied to a Polygram CEL400 Uni layer plate (Merck, Darmstadt, Germany). Electrophoretic separation of phosphoamino acids was in 10% acetic acid, 1% pyridin, pH 3.5, at 800 V for 1 h. Radioactively labelled phosphoamino acids were identified by visualization of standard phosphoamino acids with ninhydrin and autoradiography.

Preparation of tissue extracts

Bovine or rat skeletal muscle, dissected into pieces, was shock-frozen in liquid nitrogen and stored at –80°C. Then 0.5 g of material were homogenized in 3 vol of ice-cold 5 mM EDTA, 15 mM 2-mercaptoethanol pH 7.0 and the resulting suspension clarified by centrifugation (4°C, 11 000 *g*, 10 min). The supernatant was applied onto a MonoQ HR 5/5 column (Pharmacia, Uppsala, Sweden). After washing with a buffer containing 50 mM Tris–HCl pH 7.9 and 1 mM DTT, protein was eluted with a linear gradient from 0 to 500 mM KCl in the same buffer. Assays for kinase activity were performed as described above.

Myosin binding assays

α-Chymotryptic myosin subfragments (myosin rod and LMM) and recombinant LMM fragments (LMM 75, LMM 59, LMM50, LMM 50–75, LMM 30) were adjusted to 50 mM KCl, 5 mM Na phosphate pH 7.0 to allow the formation of filaments. Approximately 1 μg of each suspension was spotted onto nitrocellulose membranes (BA-85, Schleicher and Schüll, Dassel, Germany). After air drying, the strips were blocked with overlay buffer (1% bovine serum albumin, 0.2% Tween-20, 100 mM KCl, 20 mM imidazole-HCl pH 7.0, 1 mM DTT) for 30 min. Individual strips were treated for 60 min with the respective myomesin fragments in the same buffer. After three washes with overlay buffer, strips were incubated for 45 min with rat monoclonal antibody YL1/2 (Wehland *et al.*, 1984), specific for the EEF tag of our recombinant myomesin fragments. Strips were washed as described above and treated with peroxidase-conjugated goat anti-rat antibody (Dianova) diluted 1:1000 in overlay buffer for 30 min. After a final washing cycle, antibody binding was visualized by reaction in 5 ml of 100 mM Tris–HCl pH 7.5 supplemented with 100 μl of diaminobenzidine (40 mg/ml stock), 25 μl of $NiCl_2$ (80 mg/ml stock) and 1.5 μl of 30% H_2O_2. All steps were performed at room temperature.

Titin binding assay

Recombinantly expressed titin fragments (0.2 μg for each domain) were spotted on nitrocellulose membranes (BA-85, Schleicher and Schüll, Dassel, Germany) pre-wetted with phosphate-buffered saline. Blocking, incubation with T7-tagged myomesin fragments and washing was as described for the myosin binding assays (see above). Binding to titin was detected by the T7 tag-specific murine monoclonal antibody (1:1000 diluted, Novagen) followed by peroxidase-conjugated goat anti-mouse antibody (1:1000 diluted, Dianova) in overlay buffer. Visualization of antibody binding was as described for the myosin binding assay.

Miscellaneous procedures

SDS–PAGE and immunoblotting were as described (Fürst *et al.*, 1988). Protein concentrations were obtained with the BioRad dye reagent. Synthetic peptides were obtained by Fmoc chemistry on a Pep Synthesizer TM9050 (Millipore Co., Bedford, USA). HPLC analysis of synthetic peptides was performed on a Vydac 218 TP54 column at 50°C using a gradient of 0–90% acetonitrile in 0.1% trifluoroacetic acid as eluent.

Acknowledgements

Dr Alfred Wittinghofer (Max-Planck-Institute for Molecular Physiology, Dortmund, Germany) kindly provided the cDNA of rabbit myosin heavy chain 2/10. We thank Frank Steiner (this institute) for making the recombinant myosin constructs and Uwe Plessmann for expert technical assistance. This work was supported in part by grants from the Deutsche Forschungsgemeinschaft to D.O.F., M.G. and K.W.

References

Ausubel,F.M., Brent,R., Kingston,R.E., Moore,D.D., Seidman,J.G., Smith,J.A. and Struhl,K. (1987) *Current Protocols in Molecular Biology.* Wiley and Sons, Inc., New York

Casnellie,J.E. (1991) Assay of protein kinases using peptides with basic residues for phosphocellulose binding. *Methods Enzymol.*, **200**, 115–120.

Freiburg,A. and Gautel,M. (1996) A molecular map of the interactions of titin and myosin-binding protein C: implications for sarcomeric assembly in familial hypertrophic cardiomyopathy. *Eur. J. Biochem.*, **235**, 317–323.

Fürst,D.O. and Gautel,M. (1995) The anatomy of a molecular giant: how the sarcomere cytoskeleton is assembled from immunoglobulin superfamily molecules. *J. Mol. Cell. Cardiol.*, **27**, 951–960.

Fürst,D.O., Osborn,M., Nave,R. and Weber,K. (1988) The organization of titin filaments in the half sarcomere revealed by monoclonal antibodies in immunoelectron microscopy; a map of 10 non repetitive epitopes starting at the Z-line extends close to the M-line. *J. Cell Biol.*, **106**, 1593–1605.

Gautel,M., Leonard,K. and Labeit,S. (1993) Phosphorylation of KSP motifs in the C-terminal region of titin in differentiating myoblasts. *EMBO J.*, **12**, 3827–3834.

Grove,B.K., Kurer,V., Lehner,C., Doetschmann,T.C., Perriard,J.-C. and Eppenberger,H. (1984) A new 185,000-dalton skeletal muscle protein detected by monoclonal antibodies. *J. Cell Biol.*, **98**, 518–524.

Grove,B.K., Cerny,L., Perriard,J.-C. and Eppenberger,H.M. (1985) Myomesin and M-protein: expression of two M-band proteins in pectoral muscle and heart during development. *J. Cell Biol.*, **101**, 1413–1421.

Grove,B.K., Holmbom,B. and Thornell,L.-E. (1987) Myomesin and M protein: differential expression in embryonic fibers during pectoral muscle development. *Differentiation*, **34**, 106–114.

Kemp,B.E., Graves,D.J., Benjamini,E. and Krebs,E.G. (1977) Role of multiple basic residues in determining the substrate specifity of cyclic AMP-dependent protein kinase. *J. Biol. Chem.*, **251**, 4888–4894.

Laemmli,U.K. (1970) Cleavage of structural proteins during the assembly of the head of bacteriophage T4. *Nature*, **227**, 680–685.

Maeda,K., Sczakiel,G. and Wittinghofer,A. (1987) Characterization of cDNA coding for the complete light meromyosin portion of a rabbit fast skeletal muscle myosin heavy chain. *Eur. J. Biochem.*, **167**, 97–102.

Margossian,S.S. and Lowey,S. (1982) Preparation of myosin and its subfragments from rabbit skeletal muscle. *Methods Enzymol.*, **85**, 55–71.

Masaki,T. and Takaiti,O. (1974) M-protein. *J. Biochem.*, **75**, 367–380.

Nave,R., Fürst,D.O. and Weber,K. (1989) Visualization of the polarity of isolated titin molecules; a single globular head on a long thin rod as the M-band anchoring domain? *J. Cell Biol.*, **109**, 2177–2188.

Obermann,W., Plessmann,U., Weber,K. and Fürst,D.O. (1995) Purification and biochemical characterization of myomesin, a myosin and titin binding protein, from bovine skeletal muscle. *Eur. J. Biochem.*, **233**, 110–115.

Obermann,W.M.J., Gautel,M., Steiner,F., Van der Ven,P.F.M., Weber,K. and Fürst,D.O. (1996) The structure of the sarcomeric M band: localization of defined domains of myomesin, M-protein and the 250 kDa carboxyterminal region of titin by immunoelectron microscopy. *J. Cell Biol.*, **134**, 1441–1453.

Pearson,R.B. and Kemp,B.E. (1991) Protein kinase phosphorylation site sequences and consensus specifity motifs: tabulations. *Methods Enzymol.*, **200**, 62–81.

Saiki,R.K., Scharf,S.J., Faloona,F., Mullis,G.T. and Ehrlich,H.A. (1985) Enzymatic amplification of beta-globin genomic sequences and restriction site analysis for diagnosis of sickle cell anemia. *Science*, **230**, 1350–1354.

Shaw,G., Debus,E. and Weber,K. (1984) The immunological relatedness of neurofilament proteins of higher vertebrates. *Eur. J. Cell Biol.*, **34**, 130–136.

Small,J.V., Fürst,D.O. and Thornell,L.-E. (1992) The cytoskeletal lattice of muscle cells. *Eur. J. Biochem.*, **208**, 559–572.

Studier,F.W., Rosenberg,A.H., Dunn,J.J. and Dubendorff,J.W (1990) Use of T7 RNA polymerase to direct expression of cloned genes. *Methods Enzymol.*, **185**, 60–89.

Trinick,J. and Lowey,S. (1977) M-protein from chicken pectoralis muscle: isolation and characterization. *J. Mol. Biol.*, **113**, 343–368.

Vinkemeier,U., Obermann,W., Weber,K. and Fürst,D.O. (1993) The globular head domain of titin extends into the center of the sarcomeric M band. *J. Cell Sci.*, **106**, 319–330.

Wehland,J., Schröder,H.C. and Weber,K. (1984) Amino sequence requirements in the epitope recognized by the the α-tubulin-specific rat monoclonal antibody YL 1/2. *EMBO J.*, **3**, 1295–1300.

Wessel,D. and Flügge,U.J. (1984) A method for the quantitative recovery of protein in dilute solution in the presence of detergents and lipids. *Anal. Biochem.*, **138**, 141–143.

Received on August 1, 1996; revised on September 30, 1996